

# Stability Analysis of a Hexapod Robot Driven by Distributed Nonlinear Oscillators with a Phase Modulation Mechanism

Yuichi Ambe, Timo Nachstedt, Poramate Manoonpong, Florentin Wörgötter,  
Shinya Aoi and Fumitoshi Matsuno

**Abstract**—In this paper, we investigated the dynamics of a hexapod robot model whose legs are driven by nonlinear oscillators with a phase modulation mechanism including phase resetting and inhibition. This mechanism changes the oscillation period of the oscillator depending solely on the timing of the foot’s contact. This strategy is based on observation of animals. The performance of the controller is evaluated using a physical simulation environment. Our simulation results show that the robot produces some stable gaits depending on the locomotion speed due to the phase modulation mechanism, which are similar to the gaits of insects.

## I. INTRODUCTION

Humans and legged animals show an outstanding locomotive ability by using their legs. They can traverse on almost every terrain in the world even where machines using wheels or tracks cannot go. They change their gaits depending on the speed and environments, for example, four legged animals, such as horses, change their gait depending on the speed (e.g., walk, trot and gallop gaits). Insects also change their gaits (e.g., tripod and metachronal gaits). So far, many researchers investigate their gait transition to understand the mechanism of the gaits from various viewpoints.

In the field of insects, Wilson [1] pointed out from the observation that the gaits of insects seem to fulfill the following rules;

- 1) A wave of protractions (swing movements of the legs) runs from posterior to anterior (and no leg protracts until the one behind is placed in a supporting position).
- 2) Contralateral legs of the same segment alternate in phase.

and he classified the gaits in five patterns. The tripod and metachronal gaits also fulfill these rules. There are other observation results about insects. Hughes [2] showed that the gaits transit continuously in insects.

This work was partly supported by the JSPS Institutional Program for Young Researcher Overseas Visits. This work was also partly supported by Emmy Noether grant MA4464/3-1 of the Deutsche Forschungsgemeinschaft and Bernstein Center for Computational Neuroscience II Göttingen (BCCN grant 01GQ1005A, project D1) as well as by the HeKKSaGOn network.

Y. Ambe and F. Matsuno are with the Department of Mechanical Engineering and Science, Graduate School of Engineering, Kyoto University, Kyotodaigakukatsura, Nishikyo-ku, Kyoto, 615-8540, Japan [amby.yu@gmail.com](mailto:amby.yu@gmail.com)

T. Nachstedt, P. Manoonpong and F. Wörgötter are with the Bernstein Center for Computational Neuroscience, III Physikalisches Institut - Biophysik, Georg-August-Universität Göttingen, 37077 Göttingen, Germany [Poramate@Manoonpong.com](mailto:Poramate@Manoonpong.com)

S. Aoi is with the Department of Aeronautics and Astronautics, Graduate School of Engineering, Kyoto University, Kyotodaigakukatsura, Nishikyo-ku, Kyoto, 615-8540, Japan [shinya\\_aoi@kuaero.kyoto-u.ac.jp](mailto:shinya_aoi@kuaero.kyoto-u.ac.jp)

TABLE I

THE LEG  $i$ 'S "DENAVID-HARTENBERG" LINK PARAMETERS

Joint	$\theta$	$\alpha$	$l$	$d$
1	$\theta_{i1}$	$\pi/2$	$l_1$	0
2	$\theta_{i2}$	0	$l_2$	0
3	$\theta_{i3}$	0	$l_3$	0

Nowadays, many researchers try showing that this movement can be achieved by using Central Pattern Generator (CPG) [3]-[5] and neural models [6]-[8]. Previously, we also designed neural controllers using a single CPG to control hexapod robots and showed their adaptability [7][8]. Other researchers also investigated the gait transition from the points of energy consumption by making simple hexapod model. Nishii [9] showed that the gait transition in insects could be explained in the point of minimizing energy consumption under some assumptions. However, the reason why insects choose the gait which fulfills the Wilson’s rules is still not clear. This reason could be explained from the relation between neural oscillators and the robot’s dynamics.

In this paper, we design a control system by using a concept of simple phase resetting mechanism derived from observation of animals and shows that this system produces an insect-like gaits, which fulfill the Willson’s rules. The phase resetting mechanism resets the phase of the oscillation when the foot touches the ground. Aoi *et al.* [10] showed that the gait of a quadruped model changes depending on the locomotion speed (duty rate) and this transition shows hysteresis similar to animals by using this simple mechanism. Fujiki *et al.* [11] showed that the gait of a hexapod model changes depending on the locomotion speed (duty rate) and this transition also shows hysteresis. Based on this concept, we discuss what gaits are determined by numerical simulations.

The contributions of our study are as follows. We introduce a simple phase modulation mechanism which is an improvement of the phase resetting mechanism to simplify the mechanism and get a new result. Although in our previous study [11] we focused on the hysteresis property in the gait transition by assuming the symmetry between anterior and posterior part of the body, the main purpose of this paper is to investigate what gaits are produced depending on physical parameters without the assumption and to investigate their stability.

## II. HEXAPOD ROBOT

Figure 1 shows a hexapod robot model which is composed of three homogeneous modules. Each module has a regular

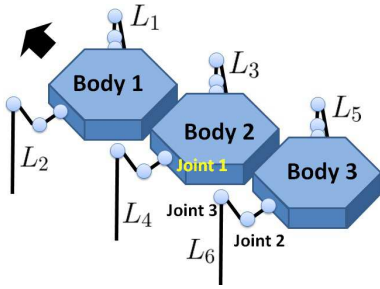


Fig. 1. Hexapod robot model

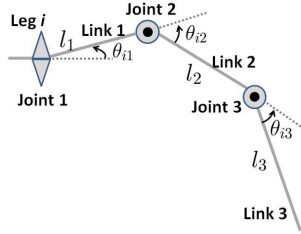


Fig. 2. Configuration of the leg

hexagonal prism body. This module is based on our previously developed robot [12]. The modules are connected to each other by stiff joints. This robot has six legs ( $L_1, L_2 \dots L_6$ ) which have three joints as shown in Fig. 2. Each joint has a servomotor and the joint angle ( $\theta_{i1}, \theta_{i2}, \theta_{i3}$  for each  $L_i$ ) is controlled by a PD controller. A touch sensor is installed on the tip of each leg. Table I shows the “Denavit-Hartenberg” link parameters [13] of each leg. Physical parameters of the robot are given in Table II.

### III. CONTROL SYSTEM

To generate robot locomotion, we construct a locomotion control system (Fig. 3). We use six CPG units and each CPG unit is used for one leg to produce phase information. We denote the phase of the CPG unit  $i$  ( $i = 1, \dots, 6$ ) as  $\phi_i$  ( $0 \leq \phi_i \leq 2\pi$ ). Each CPG unit interacts with other CPG units and is also affected by the foot contact (Fig. 4).  $\Delta_{ij} = \phi_i - \phi_j$  represents the phase difference between CPG units  $i$  and  $j$ . The leg movement is designed based on the phase of the CPG unit (Fig. 6). This leg movement is achieved by the PD-Controller of the joint angle (“Motor Controller” in Fig.3).

Figure 5 shows the details of the phase  $\phi_i$  of CPG unit  $i$ . Here, we set the duration of a stance phase as ( $0 \leq \phi_i(t) <$

TABLE II  
PHYSICAL PARAMETERS OF THE ROBOT

Link	Parameter	Value
Body	Mass [kg]	0.32
	Side[mm]	74
Leg link 1	Mass [kg]	0.05
	$l_1$ [mm]	68
Leg link 2	Mass [kg]	0.05
	$l_2$ [mm]	68
Leg link 3	Mass [kg]	0.007
	$l_3$ [mm]	114.5

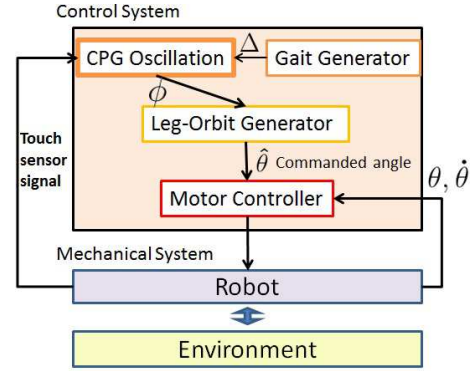


Fig. 3. Control system of the hexapod robot

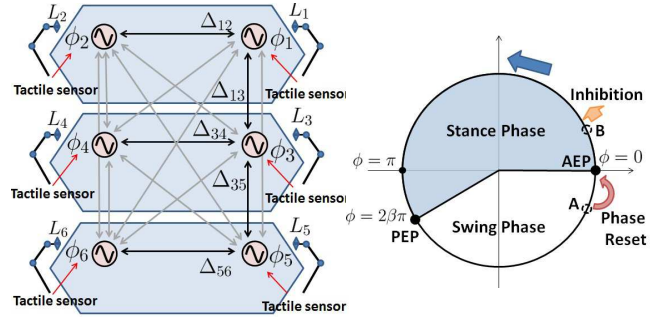


Fig. 4. CPG control network

Fig. 5. Phase of CPG unit

$2\beta\pi$ ) while the rest indicates a swing phase, where  $\beta$  is the duty rate (the ratio between the stance phase and gait cycle durations). The stance phase starts from the anterior extreme position (AEP) ( $\phi_i = 0$ ), and the swing phase starts from the posterior extreme position (PEP) ( $\phi_i = 2\beta\pi$ ). Although we designed the leg movement composed of the stance and swing phases, the leg does not necessarily contact the ground at the AEP or leave the ground at the PEP.

In the following, we show the details of our control system.

#### A. Gait generator

In this system, the phase difference  $\Delta_{ij}$  determines the gait of our robot. In general, it is sufficient to represent a gait by determining the values of  $[\Delta_{12}, \Delta_{34}, \Delta_{56}, \Delta_{13}, \Delta_{35}]$ . For example,  $[\pi, \pi, \pi, \pi, \pi]$  represents a tripod gait. In this paper, we set desired phase differences  $\hat{\Delta}_{12} = \pi$ ,  $\hat{\Delta}_{34} = \pi$  and  $\hat{\Delta}_{56} = \pi$  as constraints (we explain  $\hat{\Delta}$  later) because we concentrate on the phase differences between posterior and anterior (Wilson’s rule 1). Two variables  $[\Delta_{13}, \Delta_{35}]$  determines the gait. From now, we denote the phase differences  $\psi_1$  and  $\psi_2$  as  $\psi_1 = -\Delta_{13} = \phi_3 - \phi_1$  and  $\psi_2 = -\Delta_{35} = \phi_5 - \phi_3$ . Note that the control system of each robot module is isolated.

#### B. Phase modulation of the CPG unit

The phase dynamics of the CPG unit is described as follows:

$$\dot{\phi}_i(t) = \omega - \sum_{j=1}^6 k_c^{ij} \sin(\phi_i(t) - \phi_j(t) - \hat{\Delta}_{ij}) - k_f^i(t) + k_r^i(t), \quad (1)$$

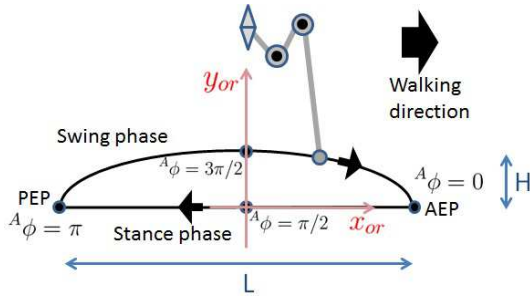


Fig. 6. Designed leg movement

$$k_f^i(t) = \begin{cases} k_{fo}\phi_i(t_o^i) & (t_o^i \leq t < t_o^i + t_{\text{duration}}, \\ & 0 \leq \phi_i(t_o^i) < 2\beta\pi) \\ 0 & \text{otherwise,} \end{cases} \quad (2)$$

$$k_r^i(t) = \begin{cases} -\phi_i(t_o^i)\delta(t-t_o^i) & (2\beta\pi \leq \phi_i(t_o^i) < 2\pi) \\ 0 & \text{otherwise,} \end{cases} \quad (3)$$

where  $\omega$  is a constant angular velocity,  $t_o^i$  is the time when the leg  $L_i$  touches the ground.  $t_{\text{duration}}$  is a duration of inhibition (see below) and is set to  $T_{\text{period}}/4$ , where  $T_{\text{period}}$  is a period of CPG oscillation.  $k_{fo}$  is a constant positive value.  $k_c^{ij}$  is a constant and  $k_c^{ij} = k_c > 0$  only when  $(i, j) \in \{(1, 2), (2, 1), (3, 4), (4, 3), (4, 5), (5, 4)\}$ ; otherwise,  $k_c^{ij}$  is 0.  $\hat{\Delta}_{ij}$  is the desired phase difference (see below).

In (1), the second term in the right-hand side represents the interaction among the CPG units. When we ignore the third and fourth terms, the phase difference  $\Delta_{ij}$  remains at  $\hat{\Delta}_{ij}$ . If  $k_c^{ij}$  is large enough,  $\Delta_{ij} = \hat{\Delta}_{ij}$  is fulfilled. The third term represents the inhibition of the oscillation of the CPG unit. When the leg  $i$  touches the ground during the stance phase ( $0 \leq \phi_i(t_o^i) < 2\beta\pi$ ), the speed of the oscillation decreases by this inhibition and the oscillation period increases as shown by the point B in Fig. 5. We call this mechanism ‘‘Phase Inhibition’’. The magnitude of inhibition changes depending on  $\phi_i(t_o^i)$ . This means that the inhibition increases when the foot contact is delayed. The fourth term is based on the phase resetting mechanism. When the leg  $i$  touches the ground during swing phase ( $2\beta\pi \leq \phi_i(t_o^i) < 2\pi$ ), the phase jumps to  $\phi_i = 0$ . This means that the oscillation period decreases as shown by the point A in Fig. 5. We call this mechanism ‘‘Phase Reset’’.

The combination of the phase inhibition and the phase reset is called ‘‘phase modulation mechanism’’.

### C. Leg-orbit generator

By using the coordinate and parameters in Fig. 6, the orbit of the leg tip is given by

$$x_{or}(t) = \frac{L}{2} \cos(A\phi(t)) \quad (4)$$

$$y_{or}(t) = \begin{cases} 0 & (0 \leq A\phi(t) < \pi) \\ -H \sin(A\phi(t)) & (\pi \leq A\phi(t) < 2\pi) \end{cases} \quad (5)$$

$${}^A\phi_i(t) = \begin{cases} \frac{1}{2\beta}\phi_i(t) & (0 \leq \phi_i(t) < 2\beta\pi) \\ \frac{\phi_i(t)-2\beta\pi}{2(1-\beta)} + \pi & (2\beta\pi \leq \phi_i(t) < 2\pi). \end{cases} \quad (6)$$

We note that direction of the leg-orbit is parallel to the moving direction of the robot.

In our previous studies using the phase resetting mechanism [10][11], we changed the orbit of the leg depending on the timing of the foot contact. In contrast, our method, employing the inhibition term introduced for the first time here, does not require to redesign the orbit, thereby leading to more simplicity.

## IV. SIMULATION

### A. Periodic gaits and their properties

Using a physical simulation environment, we aim to find periodic gaits and investigate their properties. To describe the state of our dynamic system, there are three variables  $(\psi_1, \psi_2, \phi_1)$ , where  $(\psi_1, \psi_2)$  determines the gait of our robot and  $\phi_1$  determines the oscillation phase.

1) *Periodic gaits*: To find periodic gaits, we used the Poincaré section. We define the Poincaré section  $S_{\phi_1}$  when the phase  $\phi_1$  is  $\pi$  as follows:

$$S_{\phi_1} = \{\mathbf{z} \in \mathbf{R}^2 \mid \phi_1 = \pi\}. \quad (7)$$

We can find a periodic gait from the fixed point on the Poincaré section.  $\mathbf{z} = [\psi_1 \ \psi_2]^T$  is the variable on  $S_{\phi_1}$ . We can denote the Poincaré map  $\mathbf{P}$  as mapping  $\mathbf{z}_n$  to  $\mathbf{z}_{n+1}$ , which is given by

$$\mathbf{z}_{n+1} = \mathbf{P}(\mathbf{z}_n), \quad (8)$$

where  $n$  corresponds to the  $n^{\text{th}}$  Poincaré section. Fixed point  $\mathbf{z}^*$  fulfills  $\mathbf{z}^* = \mathbf{P}(\mathbf{z}^*)$ .

2) *Stability properties*: To analyze the stability of the periodic gait, we investigate the maximum eigenvalue of Jacobian matrix of Poincaré map [14]. For the perturbation  $\Delta\mathbf{z}_n$  from fixed point  $\mathbf{z}^*$ , we can write

$$\mathbf{z}^* + \Delta\mathbf{z}_{n+1} = \mathbf{P}(\mathbf{z}^* + \Delta\mathbf{z}_n) \quad (9)$$

$$= \mathbf{P}(\mathbf{z}^*) + [\nabla\mathbf{P}(\mathbf{z}^*)]\Delta\mathbf{z}_n + O(\Delta\mathbf{z}_n^2), \quad (10)$$

where  $\nabla\mathbf{P}(\mathbf{z}^*) \in \mathbf{R}^{2 \times 2}$ . From (10), we obtain

$$\Delta\mathbf{z}_{n+1} = [\nabla\mathbf{P}(\mathbf{z}^*)]\Delta\mathbf{z}_n, \quad (11)$$

where we ignore higher terms. From the absolute values of eigenvalues  $\lambda_i$  of  $\nabla\mathbf{P}(\mathbf{z}^*)$ , we can find whether the fixed point is stable or not. The periodic gait is stable when

$$\max_{i=1,2} |\lambda_i| < 1. \quad (12)$$

We approximate  $\nabla\mathbf{P}(\mathbf{z}^*)$  as follows:

$$\nabla\mathbf{P}(\mathbf{z}^*) = \left[ \frac{\partial\mathbf{P}}{\partial\psi_1} \quad \frac{\partial\mathbf{P}}{\partial\psi_2} \right], \quad (13)$$

$$\frac{\partial\mathbf{P}(\mathbf{z}^*)}{\partial\psi_i} = \frac{\mathbf{P}(\psi_1, \dots, \psi_i + \Delta\psi, \dots) - \mathbf{P}(\psi_1, \dots, \psi_i - \Delta\psi, \dots)}{2\Delta\psi}. \quad (14)$$

Here, we used  $\Delta\psi = 0.05$ .

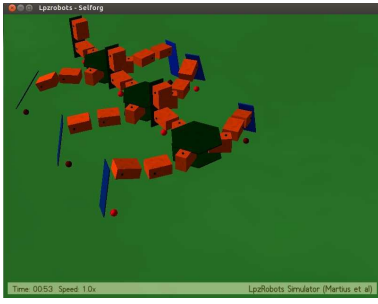


Fig. 7. Hexapod robot model in the simulation

TABLE III  
SIMULATION PARAMETERS

Parameter	Value	Parameter	Value
$k_c$	0.05	Height of leg-orbit $H$ [mm]	6
$k_{fo}$	0.1	Length of leg-orbit $L$ [mm]	10
Control frequency [Hz]	3200	Simulation frequency [Hz]	3200

### B. Simulation of a robot gait

We conducted the computer simulation by using a software LPZROBOTS<sup>1</sup> (see Fig. 7). Table III shows the parameters for the simulation. We used large values for the gain parameters of the PD-Controller to produce the designed leg movements.

## V. RESULT

### A. Periodic gaits and their properties

We investigated the dependence of the gait of our robot on the duty rate  $\beta$  (it corresponds to the locomotion speed of the robot), using  $\omega = 0.3\pi$  rad/s. For each duty rate, we performed the simulation for 30 periods and got the fixed phase differences  $\mathbf{z}^{cnv} = [\psi_1^{cnv}, \psi_2^{cnv}]$  on the  $S_{\phi_1}$ .

Figure 8 shows the results of  $[\psi_1^{cnv}, \psi_2^{cnv}]$  for the duty rate. There are two sets of  $[\psi_1^{cnv}, \psi_2^{cnv}]$  for each duty rate and they are distinguished by colors and shapes of the points. Figure 9 shows the maximum absolute eigenvalue of fixed points. The maximum eigenvalues are less than 1, which means that the periodic gaits are stable. Figures 10 and 11 show the foot print diagrams of these two gaits for  $\beta = 0.5$  and  $0.7$ , respectively.

From Figs. 8 and 9, we found that this system mainly has two periodic stable gaits (which are represented in upper fixed points (“red cross-mark”) and lower fixed points (“green x-mark”)) at each duty rate. The lower fixed points are stable at each duty rate from Fig. 9. The fixed point changes almost linearly depending on the duty rate  $\beta$  while the values  $\psi_1^{cnv}$  and  $\psi_2^{cnv}$  are almost same as shown in Fig. 8. In detail, the phase differences between hindleg and middle leg  $\psi_1^{cnv}$  and between middle leg and foreleg  $\psi_2^{cnv}$  are same and almost equal to the duration of swing phase  $2(1 - \beta)\pi$  (Note that the duty rate in converged gait is a little bit different from the nominal duty rate  $\beta$  because we use the

<sup>1</sup>It is based on the Open Dynamics Engine (ODE). For more details of the LPZROBOTS simulator, see <http://robot.informatik.uni-leipzig.de/software/>.

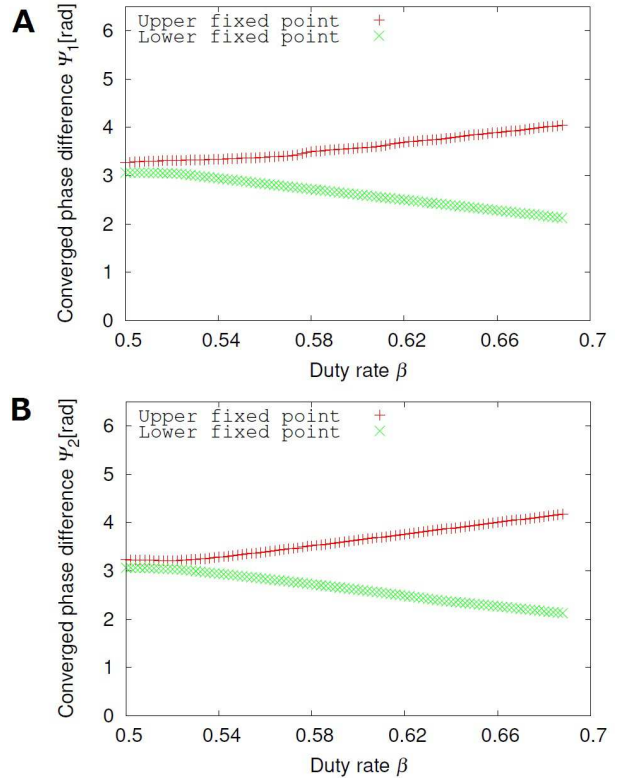


Fig. 8. **A** and **B** show the phase differences  $\psi_1^{cnv}$  and  $\psi_2^{cnv}$ , respectively. We found two fixed points for each duty rate. The red cross mark represents the upper fixed points, and the green x mark represents the lower fixed points.

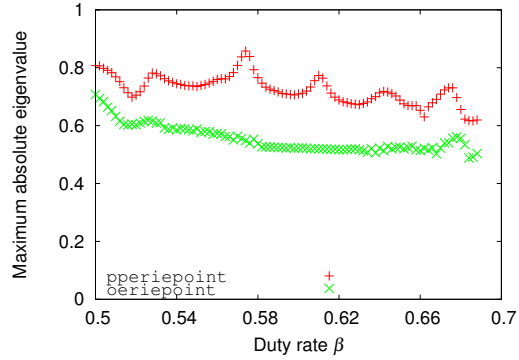
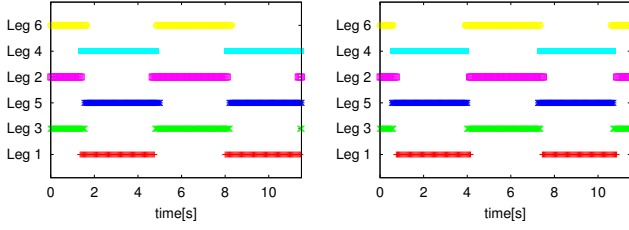


Fig. 9. Maximum absolute eigenvalue of two fixed points for the duty rate. The color and shape of the points correspond to those of Fig. 8.

phase modulation mechanism). Because of these features, the resultant gaits seems to fulfill the following rule.

- The middle leg (foreleg) leaves ground just after the hindleg (middle leg) touches ground

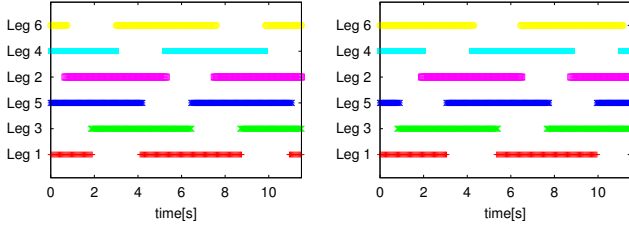
We can find from this rule that the gait fulfills the Wilson’s rule 1 at each duty rate and the gaits change continuously as observed in Hughes [2]. For  $\beta = 0.5$ , the result of  $(\psi_1^{cnv} = 3.0$  rad and  $\psi_2^{cnv} = 3.0$  rad) looks like “tripod gait” of insects as shown in Fig. 10A. As the duty rate increases (this means that the locomotion speed decreases), the gait changes gradually and finally to “metachronal gait” of insect as shown in Fig. 11A. The upper fixed points are also stable at each duty rate from Fig. 9. However, these absolute eigenvalues are larger than those of the lower fixed points. The fixed point



**A** fixed point [3.0, 3.0]

**B** fixed point [3.2, 3.2]

Fig. 10. Foot print diagram for  $\beta = 0.5$ . The line means that the leg is on the ground. **A** represents the lower fixed point and **B** represents the upper fixed point. The gait patterns look like “tripod gait”. In “tripod gait”, three legs are in the stance phase and the other three legs are in the swing phase at almost any timing.



**A** fixed point [2.0, 2.0]

**B** fixed point [4.1, 4.2]

Fig. 11. Foot print diagram for  $\beta = 0.7$ . The line means that the leg is on the ground. **A** represents the lower fixed point and **B** represents the upper fixed point. The gait pattern of **A** looks like “metachronal gait” and fulfills the Willson’s rules. In “metachronal gait”, four legs are in the stance phase and the other two legs are in the swing phase at almost any timing while fulfilling the Willson’s rules.

changes almost linearly depending on the duty rate  $\beta$  and the values  $\psi_1^{cnv}$  and  $\psi_2^{cnv}$  are almost same as Fig. 8. In detail, the phase differences between hindleg and middle leg  $\psi_1^{cnv}$  and between middle leg and foreleg  $\psi_2^{cnv}$  are same and almost equal to the duration of stance phase ( $2\beta\pi$ ). Because of these features, the resultant gaits seems to fulfill the following rule in contrast to that of lower fixed points.

- The hindleg (middle leg) leaves ground just after the middle leg (foreleg) touches ground

This means that a wave of swing movement runs from anterior to posterior. For  $\beta = 0.5$ , the result of ( $\psi_1^{cnv} = 3.2$  rad and  $\psi_2^{cnv} = 3.2$  rad) looks like “tripod gait” of insects as shown in Fig. 10B. However, as the duty rate increases, the gait changes gradually and finally to something like inverse “metachronal gait” of insect as shown in Fig. 11B. These gaits do not fulfill the Willson’s rule.

These two different gaits (lower and upper fixed points) are almost axially symmetric to the line  $\psi_i = \pi$  in Fig. 8. An interesting thing is that we could get the stable gaits only from the interaction between CPG and robot’s dynamics, and the gait which fulfills the Willson’s rules (lower fixed point) is more stable than the gaits which do not fulfill the Willson’s rule.

## B. Discussion of stability mechanism

1) *Overview*: In this subsection, we discuss how this system establishes stable insect-like gaits. Note that this

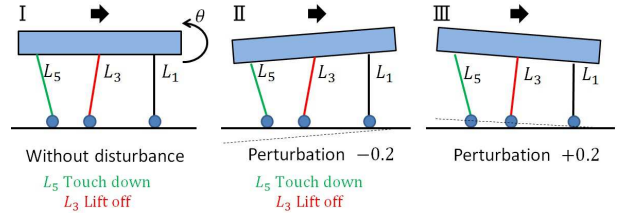


Fig. 13. The conditions of the robot when  $L_5$  touches the ground in event B on sagittal plane. In condition I,  $L_5$  just touches down the ground and  $L_3$  will lift off at once. In condition II, because of the perturbation,  $L_5$  touches the ground when the  $L_3$  starts swing movement and the body tilts as shown in the figure. In condition III,  $L_5$  touches the ground when the  $L_3$  does not lift off yet and the body tilts to other direction.

TABLE IV  
DATA OF THE SIMULATION

	$\Delta$	$\phi_i(t_o^i)$ [rad]	$\theta(t_o^i)$ [ $10^{-3}$ rad]
A	0	0.255	-1.99
	+0.2	0.261	-1.81
	-0.2	0.261	-1.66
B	0	0.255	-0.354
	+0.2	0.253	-0.470
	-0.2	0.256	-0.299
C	0	0.255	1.63
	+0.2	0.316	-0.340
	-0.2	0.154	6.96

discussion is not enough for explaining the reason why the phase differences converge to some fixed points, we just point out the possibilities of the reason. In future, we will give a good explanation about it.

We use the parameters;  $\beta = 0.65$  and the others are same as in section V-A and focus on the gait of the lower fixed point. In the following, we explain the mechanism of stability by disturbing only  $\psi_2^{cnv}$  on the Poincaré section. We also only think the movement of the legs ( $L_1$ ,  $L_3$  and  $L_5$ ) on the sagittal plane because we assumed that the contralateral legs of the same segment alternate in phase. According to the results of simulation (V-A), we can divide the periodic gait to seven phases on sagittal plane depending on stance conditions as Fig. 12. To discuss the stability, we focus on only three marked events (A, B and C on Fig. 12) because the phase modulation mechanism influences the locomotion dynamics only when the legs touch ground.

The simulation results are shown in Table IV, where we disturbed  $\psi_2^{cnv}$  on the Poincaré section (perturbation  $\Delta = 0, \pm 0.2$ ), and we show the result for each event during one periodic walking. In Table IV,  $\phi_i(t_o^i)$  is the oscillator phase of leg  $i$  when leg  $i$  touches ground and  $\theta$  is the pitch angle of the robot as shown in Fig. 13.

2) *Event A*: In this case, the  $L_3$  touches down and  $L_1$  lifts off. The phase  $\phi_3(t_o^3)$  was disturbed from 0.255 rad to 0.261 rad, which was small. Because the pitch angle was not so disturbed, the timing of the foot contact of  $L_3$  was not also disturbed. This means that the magnitude of inhibition which is applied to  $\phi_3$  was not disturbed. Therefore,  $\Delta$  did not induce changes in the gait through this event.

3) *Event B*: In this case, the  $L_1$  touches down. The phase  $\phi_1(t_o^1)$  was not so disturbed and the same discussion as the event A can apply to this event.

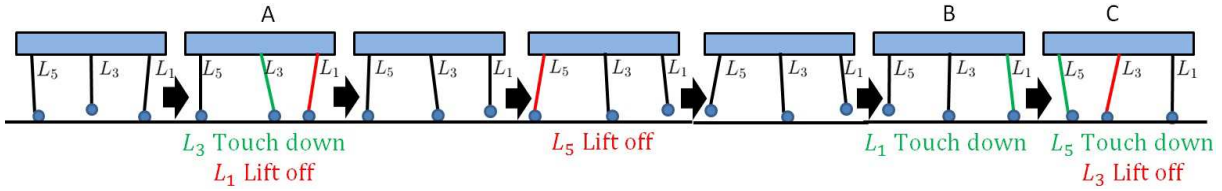


Fig. 12. Stance configurations of the periodic gait on the sagittal plane.

4) *Event C*: In this case, the  $L_5$  touches down and  $L_3$  lifts off. For  $\Delta = -0.2$ , the phase  $\phi_5(t_0^5)$  is less than that for  $\Delta = 0$ . In detail, the  $L_5$  touches the ground earlier than without disturbance and  $\phi_5(t_0^5)$  became smaller, because the pitch angle  $\theta(t_0^5)$  became larger than without disturbance as Table IV and Fig. 13-II. This means that the inhibition makes the oscillation of  $\phi_5$  faster than those of  $\phi_3$  and  $\phi_1$ , and  $\psi_2 = \phi_5 - \phi_3$  becomes larger, and finally, the absolute value of  $\Delta$  became smaller as time goes by.

On the other hand, in the case  $\Delta = +0.2$ , the phase  $\phi_5(t_0^5)$  is larger than that without disturbance. In detail, the  $L_5$  touches the ground later than without disturbance and  $\phi_5(t_0^5)$  is larger than that without disturbance, because the pitch angle  $\theta(t_0^5)$  became smaller than that without disturbance as Table IV and Fig. 13-III. This means that the inhibition makes the oscillation of  $\phi_5$  slower than those of  $\phi_3$  and  $\phi_1$ , and  $\psi_2$  becomes smaller, and finally, the absolute value of  $\Delta$  became smaller as time goes by.

5) *Summarize*: As we discussed above, we showed how perturbations evolve by focusing on leg's touching down. We expect that the phase converges to the fixed point mainly because of the Event A. Although this did not fully prove the stability, our results show that the relation between the body tilt and phase modulation and the rules mentioned in section V-A are important for gait stability. This would be a good clue to clarify this phase modulation mechanism in future.

## VI. CONCLUSION

In this paper, we investigated the locomotion of a hexapod robot driven by nonlinear oscillators with a phase modulation mechanism. The simulation results revealed that the robot produces stable gaits despite this simple mechanism. In addition, the one of the two set of gaits looks like that of insects, and fulfills the Wilson's rules.

Our results seem interesting because the relation between CPG and robot's dynamics plays an important role for gait generation and stability. This would be a key for understanding the movements of insects. In future, we will make a sophisticated model to explain this phenomena and we will also verify this movement in the real environment.

## REFERENCES

- [1] D.M. Wilson, "Insect walking", *Annu. Rev. Entomol.*, Vol. 11, pp. 103-122, 1966
- [2] G.M. Hughes, "The coordination of insect movements. I. The walking movements of insects", *J. Exp. Biol.*, Vol. 29, pp. 267-284, 1952
- [3] G. Taga, Y. Yamaguchi, and H. Shimizu, "Self-organized control of bipedal locomotion by neural oscillators in unpredictable environment", *Biol. Cybern.*, Vol. 65, pp. 147-159, 1991

- [4] C.C. Canavier, R.J. Butera, R.O. Dror, D.A. Baxter, J.W. Clark and J.H. Byrne, "Phase response characteristics of model neurons determine which patterns are expressed in a ring circuit model of gait generation", *Biol. Cybern.*, Vol. 77, pp. 367-380, 1997
- [5] A.J. Ijspeert, "Central pattern generators for locomotion control in animals and robots: A review", *Neural Netw.*, Vol. 21, pp. 642-653, 2008
- [6] S. Grillner, "Biological pattern generation: The cellular and computational logic of networks in motion" *Neuron*, Vol. 52, pp. 751-766, 2006
- [7] S. Steingrube, M. Timme, F. Wörgötter and P. Manoonpong, "Self-organized adaptation of a simple neural circuit enables complex robot behaviour", *Nat. Phys.*, Vol. 6, pp. 224-230, 2010
- [8] P. Manoonpong, F. Pasemann and F. Wörgötter, "Sensor-driven neural control for omnidirectional locomotion and versatile reactive behaviors of walking machines", *Robot. Auton. Syst.*, Vol. 56, pp. 265-288, 2008
- [9] J. Nishii, "An analytical estimation of the energy cost for legged locomotion" *J. Theor. Biol.*, Vol. 238, pp. 636-645, 2006
- [10] S. Aoi, T. Yamashita and K. Tuchiya, "Hysteresis in the gait transition of a quadruped investigated using simple body mechanical and oscillator network models", *Phys. Rev. E*, 83(6):061909, 2011
- [11] S. Fujiki, S. Aoi, T. Funato, N. Tomita, K. Senda and K. Tsuchiya, "Hysteresis in the metachronal-tripod gait transition of insects: A modeling study", *Phys. Rev. E*, 88(1):012717, 2013
- [12] M. Ohira, R. Chatterjee, T. Kamegawa and F. Matsuno, "Development of three-legged modular robots and demonstration of collaborative task execution" *In Proc. of IEEE Int. Conf. on Robotics and Automation*, pp. 3895-3900, 2007
- [13] J. Denavit and R.S. Hartenberg, "A Kinematic Notation for Lower-Pair Mechanisms Based on Matrices", *ASME J. Appl. Mech.*, Vol. 77, pp. 215-221, 1955
- [14] S.H. Strogatz, "Nonlinear Dynamics and Chaos - with application to Physics, Biology, Chemistry and Engineering", *Westview PRESS*, 2001